Accepted refereed manuscript of: Spyrakos E, González Vilas L, Torres Palenzuela JM & Barton ED (2011) Remote sensing chlorophyll a of optically complex waters (rias Baixas, NW Spain): Application of a regionally specific chlorophyll a algorithm for MERIS full resolution data during an upwelling cycle. Remote Sensing of Environment, 115 (10), pp. 2471-2485. https://doi.org/10.1016/j.rse.2011.05.008

Remote sensing chlorophyll *a* mapping of optically complex waters (rias Baixas, NW Spain): Application of a regionally specific chlorophyll *a* algorithm for MERIS full resolution data during an upwelling cycle

Evangelos Spyrakos [a], Luis González Vilas [a], Jesus M. Torres Palenzuela [a,*], Eric Desmond Barton [b]

[a] Remote Sensing and GIS Laboratory. Department of Applied Physics. Sciences Faculty. University of Vigo. Campus Lagoas Marcosende. 36310. Vigo. Spain

[b] Instituto de Investigaciones Marinas, C/Eduardo Cabello, 6, E-36208, Vigo, Spain

[*] Corresponding author: Tel. +34 986 812 631. Fax: +34 986 812 556. E-mail address: jesu@uvigo.es (J. M. Torres-Palenzuela).

Abstract

This study takes advantage of a regionally specific algorithm and the characteristics of Medium Resolution Imaging Spectrometer (MERIS) in order to deliver more accurate, detailed chlorophyll *a* (chl*a*) maps of optically complex coastal waters during an upwelling cycle. MERIS full resolution chl*a* concentrations and *in situ* data were obtained in three Galician *rias* (NW Spain) and the adjacent shelf, an area of extensive mussel cultures that experiences frequent harmful algal events. Regionally focused algorithms (NNRB) for the retrieval of chl*a* in the Galician *rias* optically complex waters were tested in comparison to sea-truth data and the one that showed the best performance was applied in a series of six MERIS (FR) images during a summer upwelling cycle to test its performance. The best performance parameters were given for the NN trained with high-quality data using the most abundant cluster found in the *rias* after the application of fuzzy c-mean clustering techniques (FCM). July 2008 was characterized by three periods of different meteorological and oceanographic states. The main changes in chl*a* concentration and distribution were clearly captured in the images. After a period of a strong upwelling favourable winds a high biomass algal event was recorded in an area of low SST. However, MERIS missed the high chlorophyll upwelled water that was detected below surface in the *ria de Vigo* by the chl*a* profiles, proving the necessity of *in situ* observations. Relatively high biomass "patches" were mapped in detail inside the *rias*. There was a significant variation in the timing and the extent of the maximum chl*a* areas. The maps confirmed that the spatial structure of the phytoplankton distribution in the study area can be complex. Surface currents and winds off the *rias Baixas* affected the distribution of chl*a* in the *rias Baixas*. This study showed that a regionally specific algorithm for an ocean colour sensor with the characteristics of MERIS in combination with *in situ* data can be of great help in chl*a*

monitoring, detection and study of high biomass algal events in an area affected by coastal upwelling such as the *rias Baixas*.

Keywords: Chlorophyll *a*, MERIS, algorithms, upwelling, Galician *rias*

Highlights

> We apply regionally specific chlorophyll *a* algorithms from MERIS data. >We study chlorophyll *a* distribution coupled with *in-situ* data during upwelling. >We provide more accurate chlorophyll *a* maps of optically complex coastal waters. >Images captured the main changes in chlorophyll *a* concentration and distribution. >

1. Introduction

Among ocean-colour derived data, chlorophyll *a* (chl*a*) concentration is the most used product since it provides a good estimation of phytoplankton biomass and is common to almost all taxonomic groups (Jeffrey et al., 1997). The phytoplankton community responds rapidly to environmental changes (EC, 2000), which can cause visible changes in chlorophyll in the surface waters.

The estimation of chl*a* concentration in the oceans from the first dedicated ocean colour scanner (CZCS) that launched in 1978 and operated until 1986 provided useful information on the global distribution of chl*a* but the quality of the data was limited (Robinson, 2004). The Sea-viewing Wide-Field-view Sensor (SeaWiFS), Moderate Resolution Imaging Spectroradiometer (MODIS) and the most recent Medium Resolution Imaging Spectrometer (MERIS) that succeeded CZCS are using more and narrower spectral bands and finer spatial resolution. MERIS provides data with a 300 m on-ground resolution in nadir (Full Resolution) and has a spectral resolution of fifteen bands from visible to near infra red, supporting one of the mission objectives for delicate coastal zone monitoring (Doerffer et al., 1999).

Traditionally, chl*a* is estimated using empirical algorithms based on the ratio between the radiance of blue and green light reflected by the sea. For the retrieval of chl*a* from ocean colour sensors various empirical spectral-ratio algorithms (Evans and Gordons, 1994; Muller-Karger et al., 1990; Aiken et al., 1995; McClain et al., 2004; O´ Reilly et al., 2000; Brown et al., 2008) and semi-analytical models (Garder and Steward, 1985; Garder et al., 1999) were developed. In typical case II waters, where high concentrations of water constituents (CDOM, detritus) absorb strongly in the blue

92 decoupling the phytoplankton absorbance, this ratio cannot be used for an accurate
93 retrieval of chl*a* (Morel and Prieur 1977; Gons, 1999; Gitenlson *et al.*, 2007).

94 In the effort for more accurate retrieval of water constituents in optically complex
95 waters, neural network (NN) techniques can play an important role, since they seem
96 ideal for multivariate, complex and non-linear data modelling (Thiria, 1993). In the last
97 decades the application of neural network (NN) techniques for the estimation of selected
98 water quality parameters from ocean-colour has increased (Atkinson and Tatnall, 1997;
99 Keiner and Yan, 1998; Dzwonkowski and Yan, 2005; Zhang *et al*., 2003; Shahraiyni et
100 al., 2009). Dransfeld et al., (2004) proposed that studies for development of ocean
101 colour algorithms should be regionally specific and emphasised the role of NNs in the
102 retrieval of water constituents especially in Case 2 waters. NN based algorithms are
103 currently used as standard products for the estimation of chl*a*, SPM and yellow
104 substances by the European Space Agency (ESA) for MERIS data (Doerffer and
105 Schiller, 2007, 2008).

106 Although remote sensing tools can be used with a relatively high precision at global
107 scale for the calculation of chl*a*, they are not always totally accurate in local areas
108 (Ruddick et al., 2008). Validation methods and development or expansion of chl*a*
109 algorithms for specific areas have been widely used to test and regionalize the satellite
110 products (e.g. Gons et al., 2002; Cota et al., 2004; Witter et al., 2009).

111 In the Galician *rias* (NW Spain) the interest in developing an accurate estimation of
112 chl*a* is considerable, mainly because of the economic and social importance of the
113 extensive culture of mussels, and the frequent occurrence of harmful algal events
114 (GEOHAB, 2005).

In the present paper a neural network-based chl*a* algorithm previously developed for the Galician *rias* waters (within the *rias* and for coastal waters on the continental shelf) was applied for the first time in a short series of MERIS (FR) images delivered during an upwelling cycle in order to obtain maps of chl*a*. The performance of the neural network-based chl*a* algorithm is compared to *in situ* measurements and other algorithms that are routinely used for MERIS data. The temporal and spatial distribution of the chl*a* patterns that were captured in the MERIS images using the local adapted algorithm in relation to the meteorological and oceanographic conditions in the area are also discussed.

2. Methods and data

2.1 Description of the study area

The Galician *rias* are V-like coastal formations along the northwest part of the Iberian Peninsula (Fig. 1). The *rias Baixas* constitute the southern part of the Galician *rias*. They are formed by four large coastal embayments, from north to south: *Muros y Noya*, *Arousa*, *Pontevedra* and *Vigo*, all oriented in a SW-NE direction, and characterized by strong tides. Surface area covers approximately 600 km^2 and water depths range from 5-60 m. This study focuses on three *rias* (*Arousa*, *Pontevedra* and *Vigo*), each connected to the open sea through two entrances, to the north and south of the islands located at the external part of each *ria*. The *ria de Vigo* is the longest of the *rias* whereas the *ria de Arousa* is the widest one. *Rias* vary in width from 1-3 km in their inner part to 8-12 km in their external part (Vilas et al., 2005). The main freshwater inputs in the *rias* are by rivers that located in innermost part of the *rias*.

In these highly primary productive upwelling estuarine systems (Fraga, 1981; Torres & Barton, 2007) transient increases of phytoplankton abundance, referred to as blooms,

are a frequent phenomenon occurring mainly between early spring and late fall (Fraga, 1988; Varela, 1992; Figueiras & Ríos, 1993). Sporadically, some phytoplankton blooms in the Galician *rias* are perceived as harmful with direct and indirect impacts to the mussel production that constitute an important economic activity in the area. Harmful algal events in the Galician *rias* are a well documented phenomenon. Several studies since the 1950s referred to the harmful algal events and in general to phytoplankton ecology on the Galician *rias* particularizing favourable conditions to the development of HABs, their origin, dynamic, distribution and toxicity levels (Margalef, 1956; Tillstone et al., 1994; Figueiras et al., 1994; GEOHAB, 2005), seasonal taxonomic and chemical composition of phytoplankton and picophytoplankton, "patchiness" (Figueiras & Niell, 1987; Nogueira et al., 1997; Tillstone et al., 2003). Despite the fact that an ocean colour sensor with the characteristics of MERIS is considered adequate for chl*a* monitoring and detection of HABs in coastal areas, to our knowledge the number of studies using MERIS data in the Galician rías is limited those of Torres Palenzuela et al. (2005a; 2005b) and González Vilas et al. (2011). The latter authors developed a chl*a* algorithm based on NNs and classification techniques from MERIS full resolution data for *rias Baixas* coastal waters.

2.2 Sampling regime

Two samplings were conducted in 2008 in the *ria de Vigo*. Twelve fixed stations were visited on cloud-free days (July 9 and 22). The sampling transect extended from the open sea towards to the inner part of the *ria*. Satellite data from MERIS (FR) were available for the same days. The depth of the stations ranged from 5 m inside the *ria* to 100 m outside. Triplicate water samples from surface to 3 meters were collected at each station from a sampler (3524 cm^3) for the determination of HPLC pigments and SPM.

163 2.3 *In situ* measurements

164 *In situ* chl*a* fluorescence profile was monitored by a Turner designs CYCLOPS-7
165 submersible fluorometer. Profiles of water temperature were provided by a portable
166 meter (HI 9829, Hanna instruments). The depth of the euphotic zone was established
167 with a Secchi disk. For the High Performance Liquid Chromatography (HPLC) chl*a*
168 determination, water samples (100-200mL) were filtered through 9mm diameter
169 Whatman GF/F filters and stored at -80^{o}C for two weeks, and 95% methanol was used
170 as extraction solvent for the pigments. In this study only chl*a* concentration data are
171 presented, calculated as the sum of chlorophyllide *a*, chlorophyll *a* epimer, chlorophyll
172 *a* allomer and divinyl chlorophyll *a*. An HPLC method using a reversed phase C_8 was
173 applied for the separation of the pigments. Details of pigment extraction and separation
174 are provided in Zapata *et al.* (2000).

175 Suspended particulate material (SPM) was evaluated in terms of SPM concentration and
176 percent weight of organic material (%OM). Pre-combusted (450 ^{o}C for 24 h), pre-
177 washed in 500 mL of MilliQ, 47mm Whatman GF/F filters were used. These filters
178 were then dried at 65 ^{o}C to a constant weight. Particles were collected by filtering a
179 standard volume (1000mL) of seawater samples and then rinsed with 50mL MilliQ in
180 order to remove salts and dissolved organic material. For the determination of SPM the
181 filters were dried at 65^{o}C till no weight changes were observed. The filters were then re-
182 combusted at 450 ºC for 5 h in order to obtain the inorganic suspended material (ISM).
183 The percent weight of organic material (%OM) was determined by subtracting the ISM
184 from the SPM. All the filters were weighted on a Precisa 262 SMA-FR microbalance
185 (10^{-5} g precision).

186 2.4 Oceanographic and meteorological data

Oceanographic and meteorological data off the *rias Baixas* were provided by the Spanish Port System (www.puertos.es). More specifically, wind speed (W) and direction, current data and water temperature were observed at a Seawatch buoy station located off Cape Silleiro (42° 7.8′N, 9° 23.4′W). This meteorological station was selected as fairly representative of the study area (Herrera et al., 2005). Daily upwelling index (I_W) was estimated from wind by Bakun's (1973) method:

$$I_W = - \tau_y/(\rho_W \cdot f) = - 1000 \cdot \rho_a \cdot C_D \cdot W \cdot W_y/(\rho_W \cdot f) \qquad m^3/(s \cdot km)$$

where ρ_a is the density of air (1.2 $kg \cdot m^{-3}$ at 15ºC), C_D is an empirical dimensionless drag coefficient ($1.4 \cdot 10^{-3}$ according to Hidy, 1972), f is the Coriolis parameter ($9.9 \cdot 10^{-5}$ s^{-1} at 42º latitude), ρ_W is the density of seawater (1025 $kg \cdot m^{-3}$), and W and W_y are the average daily module and northerly component of the wind.

Moderate Resolution Imaging Spectroradiometer (MODIS-Aqua) sea surface temperature (SST) daily level 2 data for July 2008 were downloaded from the website of the National Aeronautics and Space Administration Goddard Space Flight Center (NASA-GSFC) (http://oceancolor.gsfc.nasa.gov/). The 1 × 1 km resolution MODIS data were processed using MATLAB software to derive projected SST maps of the study area. The study area for the SST maps was expanded to 42-43º N and 9.3-8.3º W. The MODIS imagery contains 6 images for the dates that MERIS data were available.

2.5 MERIS data and MERIS chl*a* algorithms for Case 2 waters

2.5.1 MERIS case II Regional Processor (C2R)

MERIS Case-2-Regional Processor (C2R) (Doerffer & Schiller, 2007, 2008) is the algorithm for chl*a* that is currently used as a standard product by the European Space Agency (ESA) for Case 2 waters. The MERIS C2R processor takes advantage of the

combined NN technique to derive the optical properties of the water (absorption of pigments, yellow substance and scattering of all particles). It includes an atmospheric correction. An inverse NN is used to emulate the inverse model and a forward NN to emulate the forward model and to test if the measured spectrum is within the scope of the training set. MERIS reflectances of eight bands in the visible spectra, information about geometry and biooptical data of the water constituents are trained in the NNs. The bio-optical model used for the simulations is based on a large data set collected mainly in European waters. Among the final outputs of the algorithm is the absorption coefficient of phytoplankton pigment (a_{pigment}). Final concentration of chl*a* is calculated according to the empirical relationship between chl*a* (algal_2) and absorption coefficient (a_{pigment}) (Doerffer & Schiller, 2005):

$$\text{algal\_2} = 21 * a_{\text{pigment}}(443)^{1.04} \quad (1)$$

which permits the modification of the parameters in order to be suitable for the each study area.

2.5.2 Regional neural network for *rias Baixas* (NNRB)

Developed by González Vilas et al., (2011), this set of algorithms represents feed-forward NNs trained by supervised learning using iterative back-propagation of error for the retrieval of chl*a* from MERIS FR data. These algorithms approximate sets of different classes of water-leaving radiance reflectances data, determined after the application of Fuzzy c-means clustering techniques (FCM), to a set of appropriate chl*a* concentrations. Input variables are 11 MERIS water leaving radiance reflectance and 3 geometry values. It was found that MERIS data can be classified in 3 clusters (#1, #2 and #3) but only one could be used for the 3 different NNs that were developed for the retrieval.

234 The method performs well in the estimation of chl*a* from MERIS (FR) data in the
235 optically complex waters of the *rias Baixas* and detects perfectly the peaks of chl*a*.
236 NNRB is based on *in situ* chl*a* data collected from the *rias Baixas* during a long period
237 survey (2002-2008), covering the temporal variability of chl*a* in all the part of the *rias*.
238 In contrast with the Schiller and Doerffer algorithm, this algorithm does not use
239 simulated data. The result is a narrower range (0.03-7.73 mg m^{-3}), but this is considered
240 as sufficient for the study area.

241 2.5.3 Application of chl*a* algorithms to MERIS imagery

242 The MERIS satellite imagery used in this study contains 6 full-resolution level-1b
243 images derived from the area in July 2008. MERIS overpasses were within 2 hours of
244 the time that samples and data were collected *in situ*. Beam 4.2 (Brockmann Consult
245 and contributors, Germany) software was used for the analysis of the imagery.

246 The BEAM-4.6´s smile correction was applied to the original level-1b data. For the
247 atmospheric correction the ocean colour data were processed with a NN-based
248 algorithm which was developed by Doerffer and Schiller (2008). The level-2 products
249 of the chl*a* concentrations calculated by the NNRB and the MERIS Case 2 Regional
250 Processor (C2R) were processed with the same atmospheric correction. This NN
251 algorithm for dedicated atmospheric correction over turbid case 2 waters is based on
252 radiative transfer simulations. The performance test of the atmospheric correction
253 showed increasing uncertainty with decreasing values of water leaving radiance
254 reflectances (Doerffer & Schiller, 2008).

255 The flags for coastline, land, clouds and invalid reflectance were raised using the Beam
256 software. Ocean colour data derived from areas significantly affected by sun glint

257 (beyond a solar zenith angle limit of 60^{o}) were characterized invalid and removed from
258 the analysis.

259 The FCM algorithm that was proposed by González et al., (2011) was applied to the l2
260 data in order to identify the different clusters. Classification images were then obtained
261 for the available MERIS images using the same FCM algorithm. The pixels in these
262 images were assigned to the cluster with the highest value in its corresponding
263 membership function and the percentage of pixels belonging to each cluster was
264 computed. The performance of the available algorithms was then tested and the NN
265 with the best performance measures was applied to the MERIS leaving radiance
266 reflectance values in order to deliver the chl*a* maps for the study area.

267 *In situ* chl*a* data points delivered from cloud-free scenes and areas that were not flagged
268 for coastline and invalid reflectance were considered to be valid match-up data and were
269 used for the performance testing of the chl*a* algorithms. Water-leaving radiance
270 reflectances and chl*a* concentrations were computed as mean values of the pixel
271 corresponding to the sampling station location and the 8 surrounding pixels. These 9
272 pixels cover approximately 0.8 km^2 of surface area and it was considered that this
273 averaging was able to reduce MERIS instrument noise. For each sampling point, the
274 number of pixels included in the median computation was also extracted as a quality
275 flag, ranging from 9 (highest quality) to 1 (lowest quality). Low quality values indicate
276 that the sampling station is located in the proximity of the coast or cloudy or foggy
277 areas, so that the reflectance values could be affected.

278 The imagery was then remapped using the standard Mercator projection with a fixed
279 grid of 890 by 890 pixels. Each chl*a* image ranges from 42^{o} 04' N to 42^{o} 40' N latitude
280 and from 8^{o} 32'W to 9^{o} 32'W longitude, which covers approximately 3.1 x 10^3 km^2.

281 2.6 Performance measures

282 The following statistical measurements were used to evaluate the performance of the
283 chl*a* models. For the measured chl*a* concentration (Chl*x*) and the modelled chl*a* (Chl$\hat{x}$)
284 the difference

285 $$PE_i = Chlx_i - Chl\hat{x}_i \qquad (2)$$

286 was noted and was used to obtain the root mean square error (RMS error) and the
287 relative RMS error, which are defined as:

288 $$RMS\ error = \sqrt{\frac{\sum_{i=1}^{N} {PE_i}^2}{N}} \qquad (3)$$

289 $$Rel.RMS\ error = \sqrt{\frac{RMSE}{\frac{1}{N}\sum_{i}^{N} Chlx_i}100} \qquad (4)$$

290 In addition, the coefficient of determination (R^2) was computed as a measurement of the
291 correlation between the Chl*x* and the Chl$\hat{x}$. RMSE and relative RMSE were used in this
292 work as measurements of absolute error (in mg m^{-3}) and relative error respectively.

293 **3. Results and discussion**

294 3.1 *In situ* data

295 Sea-truthing ranges of HPLC chl*a*, SPM, percentage of inorganic matter and Secchi
296 disk depth for the two samplings are given in Table 1, which also summarizes
297 information about the available MERIS imagery. Water temperatures near surface
298 ranged from 16.90 to 19.54 ^{o}C and from 16.58 to 18.91 ^{o}C, respectively, for the two
299 samplings. Temperature at 10 m depth during the first sampling was between 15.33 and
300 17.70 ^{o}C, whereas temperatures dropped to 13.50-14.47 ^{o}C at the sampling stations on
301 July 22.

302 Water temperature decreased from the outer part towards the inner part of the *ria*.
303 Values of Secchi disk depth between 2 to 12 m were measured in the *ria de Vigo*,
304 generally less than half the water column depth.

305 Chl*a* concentration in the surface water samples did not show a wide variation. Chl*a*
306 levels were relatively low in comparison with the temporal pattern proposed for the *rias*
307 *Baixas* by Nogueira et al. (1997) where chl*a* concentrations close to 5 mg m^{-3} are
308 described as typical during the summer period. Mean chl*a* determined by HPLC varied
309 from 0.03 at station 12 to 2.65 mg m^{-3} in the inner part during the first sampling. On
310 July 22 the highest chl*a* concentration (2.72 mg m^{-3}) was recorded in the innermost *ria*
311 station. Although the range in the surface chl*a* concentration was similar in both
312 samplings, differences were observed in the chl*a* profiles. In the sampling conducted on
313 July 9, small differences were observed in the chl*a* concentration profiles in the first 10
314 m of the water column in all stations except the three at the inner part of the *ria* where a
315 chl*a* maximum was recorded at 4 m depth (Fig. 2A). On the other hand, a vertical
316 gradient of chl*a* was detected in almost all sampling stations during the second sampling
317 (Fig. 2B), with the highest values of chla (up to 16 mg L^{-1}) found close to 10 m. The
318 same vertical distribution pattern during the month of July in *ria de Pontevedra* is
319 described in Varela et al. (2008) and is imputed to the presence of upwelled waters.

320 SPM concentrations varied from 1.17 to 3.15 mg L^{-1} in the *ria de Vigo* and showed
321 decreasing values with distance from st. 1, which is located in the inner, narrow part of
322 the *ria* and closer to the main freshwater inputs. In this part of the *ria* sediment
323 resuspension and continental runoff is probably higher having as a result high
324 concentrations of SPM.

The results of the Chl*a* and SPM analyses of this study combined with available unpublished data from the same sampling stations using the same methodology showed that these two variables vary independently (Fig. 3, determination coefficient of linear relationship R^2=0.1). This confirms the initial assumption that *rias Baixas* waters can be categorized as Case 2 (Morel & Prieur, 1977). This classification is not always a simple distinction of coastal and oceanic waters as Morel and Maritonema (2001) describe in a later study using a new dataset of optical properties, indicating the need for models more restricted in geographical and seasonal terms.

3.2 Classification results and comparison of MERIS chl*a* algorithms with *in situ* data

Classification images, showing the cluster value for each sea pixel, were obtained for the MERIS images involved in the analysis (Fig. 4). In theory, the membership grades for each cluster would allow us to blend the chl*a* concentration, obtained from the different neural networks developed for each cluster, into a given pixel, so that chl*a* maps with soft transitions would be created (Moore et al., 2009). In practice, the NNRB model was only developed for Cluster#1 (González Vilas et al., 2011), so that these classification images presented here were only useful for detecting the zones where Cluster#1 is the dominant cluster and therefore the areas where NNRB can be best applied to obtain more reliable results. Figure 4 shows that Cluster#1 is dominant in almost all the images in the rias Baixas and the adjacent area. Table 2 shows the percentage of pixels belonging to each cluster for each image over the *rias Baixas*. Cluster#1 includes the majority of the pixels in *ria de Vigo*, with more than 72% of pixels in the six images. On average, 71% and 65% of the pixels over *ria de Pontevedra* and *ria de Arousa* belong to this cluster. Cluster#2 is the predominant one in in the *ria de Pontevedra* and *ria de Arousa* in the image delivered on July 29. Cluster#3 is the least abundant in most of the images, with less than 3.25% of pixels in all of them.

However, the presence of Cluster#2 and Cluster#3 does not prevent the continuous chlorophyll mapping over large areas in the *rias*, because of the predominance of Cluster#1. The image delivered on the July 29 is more problematic (referring to the high percentage of pixels belonging to Cluster#2), although the mapping of a large part of *ria de Vigo* and small parts of ria de Pontevedra and *ria de Arousa* was possible.

Insofar as the two cloud-free field campaigns were designed specifically to collect samples within a time period of 2 hours from the MERIS overpasses time, 24 valid data were available to test performance of the MERIS chl*a* algorithms. The performance parameters for the match-up data of MERIS chl*a* retrieved by the C2R processor and the three NNRB algorithms (NNRB#1, NNRB#2 and NNRB#3) are shown in Table 3. The available dataset did not show a wide range of environmental variation, with chl*a* ranging from 0.03 to 2.72 mg m^{-3}. The three NNRB algorithms outperformed the C2R showing higher R^2 and lower RMSE values. However, the NNRB for the Cluster#1, high quality data produced well correlated results (R^2=0.70) which are much higher than the CR2 results. Bottom effects on the reflectance or the presence of macroalgae and adjacency effects might be the factors responsible for the difference in the performance parameters that was observed between NNRB#1(2) and NNRB#3. The C2R has shown good results for chl*a* retrieval in coastal areas and inland waters (Peters, 2006; Odermatt et al., 2010) but the correlation with the *in situ* data in this study was poor. The poor correlation shown by C2R may be the result of the low chl*a* concentrations that were recorded in the *ria de Vigo*. C2R is more likely to be inaccurate in low chl*a* concentrations with moderate values (>2 mg m^{-3}) of SPM (Doerffer and Schiller, 2007). Further error may arise from sea bottom reflection especially in the innermost part of the *ria*. The good performance of NNRB#3 is not surprising considering that NNRB#3 can clearly follow the cycle of chlorophyll recorded in the *rias Baixas*: concentrations

375 lower than 1 mg m^{-3} during the winter months, up to 8 mg m^{-3} during the spring and
376 autumn maxima and close to 5 mg m^{-3} during the summer. Moreover, the NNRB
377 algorithm is trained with MERIS and *in situ* chl*a* data during upwelling events.
378 NNRB#3 seems to be robust and ideal for the *rias Baixas* coastal waters where it can be
379 used for a more accurate mapping of chl*a* in order to improve the understanding of the
380 spatial and temporal distributions.

381 3.3 Upwelling cycle

382 Different meteorological and oceanographic periods were identified and categorized as
383 three different states in the area during July of 2008 (Table 4, Fig. 5). The states lasted
384 from nine to eleven days which is typical in an upwelling cycle in the area (Nogueira et
385 al., 1997).

386 *State 1 (July 1-11)*

387 This 10 d period state comes after a strong upwelling that occurred in the area at the end
388 of June (Fig. 5A) and it is characterized mainly by weak winds of variable direction
389 which are typical of upwelling relaxation in the area (deCastro et al., 2004). An
390 exception of strong downwelling-favourable wind from the south was recorded on July
391 4.

392 Surface flow off the *rias* had a northward direction with a speed ranging between 0.5
393 and 7.5 cm s^{-1} (Fig. 5B). On July 3, SST ranged between 16-17 ^{o}C inside the rias, but an
394 area with temperature higher than 17 ^{o}C was observed outside the *rias*. In the next SST
395 image (July 9) an increase in temperature was recorded in the *rias Baixas* and the
396 adjacent area (Fig. 6). The temperature increase was confirmed by the Seawatch data
397 (Fig. 5C). The daily mean water temperature off the *rias Baixas* increased from 16.4 ^{o}C,
398 in the first days of July up to 18 ^{o}C in a period of 10 days after the upwelling.

399 Two MERIS (FR) images (Fig. 7) from the study area were available during state 1, one
400 on July 3 and the other on July 9. In both, several high chl*a* "patches" were mapped
401 inside and in the outer parts of the *rias*. In the area off the external coast of the *rias* the
402 chl*a* concentration in the images remained at levels close to 0 mg m^{-3}. This pattern of
403 the phytoplankton biomass principally confined in the *rias* while in neighbouring shelf
404 area the chl*a* levels remained very low, seems to be generated by the northward flow of
405 surface waters outside the *ria*. The development of northward currents in the relaxation
406 following intense north winds, responsible for the upwelling recorded at the end of
407 June, may introduce water of high chl*a* to the three *rias* from the ocean area outside
408 them in the first days of July. The continuing mainly north-westward directed transport
409 over several days may have been responsible for the chl*a* distribution observed on July
410 9, where chl*a* concentration was significantly higher in the *ria de Arousa* than in the
411 other two *rias* in the south.

412 Different patterns of the higher chl*a* areas in the *rias* were mapped during state 1. On
413 July 3, areas of high chl*a* concentrations were mapped in the *ria de Arousa* (3-4.5 mg
414 m^{-3}) and close to the mouths of the three *rias* (higher than 2 mg m^{-3}). On July 9, chl*a*
415 concentrations greater than 2 mg m^{-3} were mapped mainly in the middle and inner parts
416 of the *ria de Vigo* and in the outer part of the *ria de Arousa*.

417 In the image obtained on July 3, areas of high chl*a* concentrations were observed in the
418 outer part of the three *rias*, whereas chl*a* decreased towards the inner part of the *rias*.
419 Varela *et al*. (2008) reported that this gradient is common in the *ria de Pontevedra*
420 during the upwelling period when the meteorological forcing is the main factor
421 responsible for the circulation of the *ria*.

Six days after the first available image, the gradient of chl*a* in the *rias* described above was observed only in the *ria de Arousa*. On the contrary, *Vigo* and *Pontevedra* were characterized by a chl*a* gradient where concentration increased toward inshore. In the *ria de Pontevedra* areas of higher chl*a* were recorded at the innermost part and close to the northern mouth of the *ria*. In the rest of the *ria de Pontevedra* chl*a* concentration was close to 0 mg m^{-3}. In the inner part of *ria de Vigo*, MERIS chl*a* varied between 2 and 3 mg m^{-3}. MERIS data delivered from areas like the most interior, shallow part of the *rias* normally considered as suspicious because the high abundance of macroalgae increases the chl*a* signal (Gons et al., 1999) were here characterized as reliable, since they were confirmed by *in situ* data. Moreover, water transparency in the 20 m station (St. 1) as determined by the Sechhi disk measurements during the first campaign was 2 meters, decreasing the effect of the bathymetry. This part of the *rias* can be firmly considered as estuary and during nutrient enrichment from river flows, high concentrations of chl*a* have been recorded (Evans and Prego, 2003). In this case the observed relatively high concentrations of chl*a* at the inner part of the two southern *rias* may be the result of the mixture of estuarine water with Eastern North Atlantic Central Water (ENACW) combined with high residence times. The different offshore-inshore gradient of *ria de Arousa* seems to be formed by material transferred to the north from the *rias de Vigo* and *Arousa* due to the northward surface currents. Differences in topography and local winds should also be considered as possible factors for the observed differences. *Ria de Arousa* is considered to be the most productive of the *rias Baixas* (Bode and Varela, 1998). In the classification of Vidal-Romaní (1984) *ria de Arousa* is categorized as open bay, while *ria de Pontevedra* and *ria de Vigo* as fjiord-like. Though fjords have deep quiescent interiors, only intermittently renewed, and a

446 shallow sill at the entrance, while the rias are shallow and have a 2 layer circulation that
447 reverses between up and downwelling.

448 *State 2 (July 12-21)*

449 State 2 was characterized by 9 d of sustained upwelling favourable winds (Fig. 5A) and
450 southwest currents of up to 6 cm s^{-1} (Fig. 5B). SST maps showed that temperature
451 ranged between 16-17 ^{o}C in the coastal area outside the *rias* (Fig. 6). Temperature
452 recorded by the Seawatch buoy decreased more than 1 ^{o}C during the upwelling (Fig.
453 5C).

454 The two chl*a* maps (Fig. 7) for this state trace the primary results of the upwelling
455 favourable winds. On July 16 map areas with the highest chl*a* concentrations were
456 recorded in the middle part of *ria de Pontevedra*, at the mouth of *ria de Arousa* and
457 through the entire *ria de Vigo*. The distributions were similar in form in the *ria de Vigo*
458 and *ria de Pontevedra* but higher chl*a* (>2.5 mg m^{-3}) was found in the former.
459 Unpublished data showed the outflow of *ria* water towards offshore in speeds that
460 reached 4 cm s^{-1}. This situation of the surface water being advected offshore in the *rias*,
461 when upwelling favourable wind started to blowing off the *rias Baixas* is typical of the
462 positive estuarine circulation that has been described in the area (Fraga and Margalef,
463 1979; Figueiras and Pazos, 1991). In this two-layer circulation, the offshore surface
464 Ekman-transport advects the low salinity water out of the *ria*, while the denser upwelled
465 water flows into the *ria* along the sea bed. The zone of enhanced surface chl*a*
466 concentration that in the MERIS images extends throughout the *ria de Pontevedra* and
467 *ria de Vigo* is probably surface water that is flowing out of the *rias* due to the positive
468 estuarine circulation generated during the upwelling favourable conditions.

469 The July 19 chl*a* image shows a noticeable increase in chl*a* with concentrations higher
470 than 1 mg m^{-3} over the entire continental shelf zone, although chl*a* decreased slightly
471 within the *rias*. In the study of Ospina-Álvarez et al. (2010) it was found out that during
472 the upwelling favourable conditions that characterized the Northern Galician *rias* during
473 the period July 13-22 2008 the ENACW did not enter in the *rias*. While in that period
474 chla in the Northern Galican *rias* did not exceed the value of 1 mg m^{-3} (Ospina-Álvarez
475 et al. 2010), in the *rias Baixas* it was generally higher than 1 mg m^{-3}, confirming the
476 suggestion that there is a difference between Northern and Western (*rias Baixas*)
477 Galician *rias* with respect to their eutrophication status under the same meteorological
478 conditions.

479 State 3 *(July 22-31)*

480 As a result of the strong upwelling event a peak of chl*a* with concentrations up to 5 mg
481 m^{-3} was mapped on July 22 in the coastal area off Galicia. The high chl*a* concentration
482 was extended from the northern offshore area to the interior of the *rias* (Fig. 7). A
483 coincident area of relatively low temperature was mapped in the north part of the study
484 area, whereas an area of warmer water was detected at the south. Differences up to 2 ^{o}C
485 were obtained between the *rias* (Fig. 6). This alongshore difference probably reflects
486 the persistence of stronger coastal upwelling in the north after the event of 10-21 July
487 and an earlier onset of relaxation in the south. It is often the case that upwelling is more
488 persistent in the north of the area (Torres and Barton, 2007). Figure 8 shows the
489 development of the upwelling on the Galician coast. With the abrupt decrease of
490 upwelling-favourable to zero wind on July 22, currents at the Seawatch buoy became
491 briefly northward as expected, but subsequently returned to southward despite the onset
492 of intermittent northward winds. The last MERIS image (July 29) is consistent with
493 strong relaxation: the offshore region has near-zero chlorophyll and a region of

494 moderately high chla is bound to the coast. Within the *rias* values tend to be low,
495 reflecting downwelling conditions. It seems probable that flow more inshore of the
496 Seawatch buoy was northward and convergent to shore. At the end of July chl*a* in the
497 *ria de Vigo* showed the lowest concentration of all the images of previous days.

498 The high chl*a* concentrations along the Galician shelf coupled with low SST. MERIS
499 and MODIS images at the start of this state on July 22 show clearly the presence of a
500 cold, chlorophyll-rich area resulting from the previous 10 d of upwelling. Although high
501 chl*a* water was recorded below the surface in the *in situ* profiles (Fig.2B) during the
502 second sampling in the *ria de Vigo*, MERIS data recorded the low surface values
503 present. Figueiras and Pazos (1991) noted the presence of nutrient-rich water during a
504 summer upwelling event in the *rias Baixas* that did not reach the surface, As soon as
505 upwelling ceases, the 2-layer circulation reverses and surface waters flow inwards and
506 sink to the lower layer carrying with them the higher surface concentrations of Chl*a*.
507 The possible non uniformity of the Inherent Optical Properties (IOP) in the water
508 profiles (Stramska and Stramski, 2005) and the development and validation of the water
509 constituent algorithms based on water samples from certain depths (e.g. O'Reily et al.,
510 2000; González Vilas et al., 2011) affirms the necessity of the *in situ* data.

511 Although this high biomass area was not sampled directly, *in situ* data from the *ria de*
512 *Vigo* revealed relatively high concentrations of diatoms (mainly *Chaetoceros* spp.),
513 small flagellates (personal observation). The ASP producer *Pseudo-nitzschia* was also
514 present in the *ria de Vigo* but in relatively low concentrations. This phytoplankton
515 composition seems to be typical in the *rias Baixas* during the summer according to the
516 annual cycle of phytoplankton abundance proposed in 1987 by Figueiras and Niel.
517 Moreover, Frangopulos et al., (in press) mentioned the presence of the red-tide

518 dinoflagellate *Noctiluca scintillans* in high abundances in *ria de Vigo* during summer
519 2008.

520 **4. Summary and conclusions**

521 Three different states of meteorological and oceanographic periods were identified in
522 the area during the July of 2008. Surface currents and winds off the *rias Baixas* affected
523 the distribution of chl*a* in the *rias Baixas*. At the beginning of July (State 1) the variable
524 and weak wind and the resulting northward surface currents limited the high chl*a*
525 concentrations to the *rias* so that only low chl*a* values were found in the offshore area.
526 Differences in the topography of the *rias*, effects of local winds and transport by
527 currents between the *rias* seem to be the main factors for the observed differences in the
528 gradients of chl*a* along the *rias* between *ria de Arousa* and the two southern *rias* (*Vigo*,
529 and *Pontevedra*). MERIS images obtained during State 2 showed the first response of
530 chl*a* distribution due to the strong favourable winds that were blowing in the area. With
531 the development of strong upwelling the circulation in the *rias* is reinforced in the
532 estuarine sense so that chla increases rapidly there. After a period of six days of
533 continued upwelling, chl*a* concentrations higher than 1mg m^{-3} were observed in all the
534 area mapped according to MERIS data. State 3 commences with the appearance of a
535 high biomass algal event coincident with the area of low SST as the culmination of the
536 preceding, extended upwelling. The weak northward winds that characterized this state
537 permitted downwelling that transferred chl*a* rich water toward the *rias*. The upwelled
538 water was recorded in the chl*a* profiles in the *ria de Vigo* but was missed by the
539 MERIS. The continuing downwelling circulation resulted in decay of the bloom and
540 subduction of surface waters in the *rias* compatible with the decrease of chl*a* observed
541 in the last MERIS image. Although MERIS has a repeat interval of three days, cloud
542 cover prevented acquisition of all possible images. Nevertheless the 6 images obtained

543 in July 2008 captured the main changes in chl*a* concentration and distribution during the
544 three periods of different meteorological and oceanographic states.

545 Previous ocean colour studies by satellite sensors (CZCS, SeaWiFS, MODIS) in the
546 Western Iberian Peninsula (WIB) during an upwelling event (McClain et al., 1986;
547 Peliz and Fiuza, 1999; Joint et al., 2001; Bode et al., 2003; Ribeiro et al., 2005; Oliveira
548 et al., 2009a, Oliveira et al., 2009b) played an important role in the identification of chl*a*
549 patterns and study of harmful algal blooms and primary production but were restricted
550 to the ocean shelf because of insufficient spatial resolution. Another problem that
551 affected many of the previous satellite remote sensing application studies in the study
552 area was the failure of the algorithms used to provide reliable chl*a* data during
553 upwelling favourable conditions especially in the areas closest to the coast. Upwelling
554 waters are characterized by considerable variability in the vertical distribution of
555 phytoplankton (Brown and Hutchings, 1987) and in the optical properties (Morel and
556 Prieur, 1977). Optically active water constituents such as SPM which are brought into
557 the surface because of the strong mixing that takes place during upwelling events may
558 vary independently of the surface chl*a* as in the typically shallow estuarine Case 2
559 waters. On the other hand, the present study allows more detailed examination of the
560 chl*a* distribution in the Galician *rias* and the adjacent area during a summer upwelling
561 cycle due to the finer spatial resolution and precise atmospheric correction offered by
562 MERIS. The application of an algorithm specially developed for the study area provides
563 more accurate mapping of chl*a*, which has, for the first time to our knowledge, provided
564 surface chl*a* mapping of the interior of the *rias Baixas*. Moreover, the fine resolution of
565 MERIS in combination with the local-based algorithm permitted the detailed detection
566 of relative high biomass "patches" in the *rias* and the coastal area. There was a
567 significant variation in the timing and the extent of the chl*a* peak areas. The maps show

568 that the spatial structure of the phytoplankton distribution in the study area can be
569 complex. Some of these areas of high chl*a* that are apparent in satellite images can be
570 missed by *in situ* monitoring programmes. High chl*a* levels in the *rias* due to the
571 increase in the concentration of harmful phytoplankton species have been recorded in
572 the past especially in summer (GEOHAB, 2005). An example of a localized feature is
573 that constantly high surface chl*a* was observed in the Bay of Baiona, located in the
574 southern mouth of *ria de Vigo* in all the images (Figure 9). The Bay of Baiona is
575 characterized as the zone of *ria de Vigo* where harmful algal events due to species like
576 *Alexandrium minutum* are a frequent and recurrent phenomenon (Bravo et al., 2010). It
577 is worth noting that for the area seaward of the *rias* all the algorithms used in this study
578 came up with very similar values and patterns for chl*a*. Moreover, this study showed
579 that the synergy of two space borne sensors (MERIS, MODIS) in combination with *in*
580 *situ* data can be of great help in the monitoring, detection and study of high biomass
581 algal events in an coastal upwelling areas.

582 **Acknowledgements**

583 MERIS data were obtained through ESA/ENVISAT project AO-623. We are very
584 grateful to A. Acuña and D. Perez Estevez for their helpful assistance during the field
585 work. This work was partially funded by the European Commission's Marie Curie
586 Actions (project 20501 ECOsystem approach to Sustainable Management of the Marine
587 Environment and its living Resources [ECOSUMMER]) through a grant supported ES.

588 References
589
590 Aiken, J., Moore, G., F., Trees, C., C., Hooker, S., B., & Clark, D., K. (1995). The
591 SeaWiFS CZCS-type pigment algorithm. In, *SeaWiFS Technical Report Series* (p. 34).
592 Greenbelt MD.
593 Atkinson, P.M., & Tatnall, A.R.L. (1997). Introduction Neural networks in remote

sensing. *International Journal of Remote Sensing, 18*, 699-709.

Bezdek, J.C. (1981). *Pattern Recognition with Fuzzy Objective Function Algorithms*. New York: Plenum.

Bode, A., & Varela, M. (1998). Primary production and phytoplankton in three Galician Rias Altas (NW Spain): seasonal and spatial variability. *Scientia Marina, 62*(4), 319-330.

Bravo, I., Figueroa, R.I., Garcés, E., Fraga, S., & Massanet, A. (2010). The intricacies of dinoflagellate pellicle cysts: The example of *Alexandrium minutum* cysts from a bloom-recurrent area (Bay of Baiona, NW Spain). *Deep Sea Research Part II: Topical Studies in Oceanography, 57*, 166-174.

Brown, C., A., Huot, Y., Werdell, P., J., Gentili, B., & Claustre, H. (2008). The origin and global distribution of second order variability in satellite ocean color and its applications to algorithm development. *Remote Sensing of Environment, 112*, 4186-4203.

Doerffer, R., & Schiller, H. (2007). The MERIS Case 2 water algorithm. *International Journal of Remote Sensing, 28*, 517-535.

Doerffer, R., & Schiller, H. (2008). MERIS Regional Coastal aln Lake Case 2 Water Project - Atmoshperic Correction ATBD. In: GKSS Research Center 21502 Geestacht.

Dzwonkowski, B., & Yan, X., -H. (2005). Development and application of a neural network based ocean colour algorithm in coastal waters. *International Journal of Remote Sensing, 26*, 1175-1200.

EC (2000). Directive of the European Parliament and of the Counsil 2000/60/EC establishing a framework for community action in the field of water policy. *Official Journal of the European Communities*, L327/321.

Evans, R., H., & Gordon, H., R. (1994). Coastal zone color scanner system calibration: A retrospective examination. *Journal of Geophysical Research, 99*, 7293-7307.

Evans, G., & Prego, R. (2003). Rias, estuaries and incised valleys: is a ria an estuary? *Marine Geology, 196*, 171-175.

Figueiras, F., & Pazos, Y. (1991). Microplankton assemblanges in three Rías Baixas (Vigo, Arosa and Muros, Spain) with a subsurface chlorophyll maximum: their reletionships to hydrography. *Marine Ecology Progress Series, 76*, 219-233.

Figueiras, F.G., & Ríos, A.F. (1993). Phytoplankton succession, red tides and the hydrographic regime in the Rías Bajas of Galicia. In T.J. Smayda & Y. Shimizu (Eds.), *Toxic Blooms in the Sea* (pp. 239-244). New York: Elsevier.

Figuieiras, F.G., Jones, K.J., Mosquera, A.M., Alvarez-Salgado, X.A., Edwards, E., & MacDougall, N. (1994). Red tide assemblage formation in an estuarine upwelling ecosystem: Ria de Vigo. *Journal of Plankton Research, 16*, 857-878.

Fraga, F. (1981). Upwelling off the Galician coast North West Spain. In E. Suess. & J. Thiede (Eds.), *Coastal upwelling* (pp. 176-182`). New York: Plenum Publishing Corp.

631 Fraga, S., Anderson, D.M., Bravo, I., Reguera, B., Steidinger, K.A., & Yentsch, C.M.
632 (1988). Influence of upwelling relaxation on dinoflagellates and shelfish toxicity in Ria de Vigo,
633 Spain. *Estuarine Coastal Shelf Science, 27*, 349-361.
634 Garder, K., L., Chen, F., R., Lee, Z., P., Hawes, S., K., & Kamykowski, D. (1999).
635 Semianalytic moderate-resolution imaging spectrometer algorithm for chlorophyll a
636 concentration and absorption with bio-optical domains based on nitrate-depletion temperatures.
637 *Journal of Geophysical Research, 104*, 5403-5421.
638 Garder, K., L., & Steward, R., G. (1985). A remote-sensing reflectance model of a red-
639 tide dinoflagellate off west Florida. *Limnology and Oceanography, 30*, 286-298.
640 GEOHAB (2005). Global Ecology and oceanography of Harmful Algal Blooms
641 (GEOHAB). In G. Pitcher, T. Moita, V. Trainer, R. Kudela, F.G. Figueiras & T. Probyn (Eds.),
642 *GEOHAB Core Research Project: HABs in Upwelling Systems* (p. 82 p.). Paris and Baltimore:
643 IOC and SCOR.
644 Gigueiras, F.G., & Niell, F.X. (1987). Composición del fitoplankton de la ría de
645 Pontevedra (NO de España). *Investigación Pesquera, 51*, 371-409.
646 Gitelson, A., A., Schalles, J., F., & Hladik, C., M. (2007). Remote chlorophyll-a
647 retrieval in turbid, productive estuaries: Chesapeake Bay case study. *Remote Sensing of*
648 *Environment, 109*, 464-472.
649 González Vilas, L., Spyrakos, E., & Torres Palenzuela, J., M. (2011). Neural network
650 estimation of chlorophyll *a* from MERIS full resolution data for the coastal waters of Galician
651 *rias* (NW Spain). *Remote Sensing of Environment*, 115, 524-535.
652 Gons, H. (1999). Optical Teledetection of Chlorophyll a in turbid inland waters.
653 *Environmental Science & Technology, 33*, 1127-1132.
654 Gons, H.J., Auer, M.T., & Effler, S.W. (2008). MERIS satellite chlorophyll mapping of
655 oligotrophic and eutrophic waters in the Laurentian Great Lakes. *Remote Sensing of*
656 *Environment, 112*, 4098-4106.
657 Hornik, K., Stinchombe, M., & White, H. (1989). Multilayer feed-forward networks are
658 universal approximators. *Neural Networks, 2*, 359-366.
659 Jeffery, S., Mantoura, R., & Wright, S. (1997). *Phytoplankton pigments in*
660 *oceanography:guidelines to modern methods*. Paris, France: UNESCO Publishing.
661 Keiner, L., E., & Yan, X., H. (1998). A neural network model for estimating sea surface
662 chlorophyll and sediments from thematic mapper imagery. *Remote Sensing of the Environment,*
663 *66*, 153-165.
664 Kratzer, S., Brockmann, C., & Moore, G. (2008). Using MERIS full resolution data to
665 monitor coastal waters - A case study from Himmerfjärden, a fjord -like bay in the northwestern
666 Baltic Sea. *Remote Sensing of Environment, 112*, 2284-2300.
667 Margalef, R. (1956). Estructura y dinámica de la ´´purga de mar´´ en Ría de Vigo.

668 *Investigacion Pesquera, 5*, 113-134.
669 McClain, C., R., Feldman, G., C., & Hooker, S., B. (2004). An overview of the
670 SeaWiFS project and strategies for producing a climate research quality global ocean bio-optical
671 time series. *Deep-Sea Research II, 51*, 6-42.
672 Morel, A., Claustre, H., Antoine, D., & Gentili, B. (2007). Natural variability of bio-
673 optical properties in Case 1 waters: Attenuation and reflectance within the visible and near-UV
674 spectral domains as observed in South Pacific and Mediterranean waters. *Biogeosciences, 4*,
675 2147-2178.
676 Morel, A., & Prieur, L. (1977). Analysis of variations in ocean color. *Limnology and*
677 *Oceanography, 22*, 709-722.
678 Muller-Karger, F., E., McClain, C., R., Sambrotto, R., N., & Ray, G., C. (1990). A
679 comparison of ship and coastal zone color scanner mapped distribution of phytoplankton in the
680 southeastern Bering Sea. *Journal of Geophysical Research, 95*, 483-499.
681 Nogueira, E., Perez, F.F., & F., R.A. (1997). Seasonal patterns and long-term trends in
682 an estuarine upwelling ecosystem (Ria de Vigo, NW Spain). *Estuarine Coastal and Shelf*
683 *Science, 44*, 185-300.
684 Odermatt, D., Giardino, C., & Heege, T. (2010). Chlorophyll retrieval with MERIS
685 Case-2-Regional in perialpine lakes. *Remote Sensing of Environment, 114*, 607-617.
686 O'Reily, J., E., Maritorena, S., Siegel, D., A., O'Brien, M., C., Toole, D., & Mitcell, B.,
687 G. et al (2000). Ocean color chlorophyll a algorithms foe SeaWiFS, OC2 and OC4. In (p. 49):
688 NASA Technical Memorandum 2000-206892.
689 Robinson, I. (2004). *Measuring the Oceans from Space: The principles and methods of*
690 *satellite oceanography*. Chichester, UK: Spinger.
691 Shahraiyni, H., T., Shouraki, S., B., Fell, F., Schaale, M., Fischer, J., Tavakoli, A.,
692 Preusker, R., Tajrishy, M., Vatandoust, M., & Khodaparast, H. (2009). Application of an active
693 learning method to the retrieval of pigment from spectral remote sensing reflectance data.
694 *International Journal of Remote Sensing, 30*, 1045-1065.
695 Tillstone, M., B. M., Figueiras, F.G., & Fermín, E.G. (2003). Phytoplankton
696 composition, phytosynthesis and primery production during different hydrographic conditions at
697 the Northwest Iberian upwelling system. *Marine Ecology Progress Series, 252*, 89-104.
698 Tilstone, G.H., Figueiras, F.G., & Fraga, F. (1994). Upwelling-downwelling sequences
699 in the generation of red tides in a coastal upwelling system. *Marine Ecology Progress Series,*
700 *112*, 241-253.
701 Torres, R., & Barton, E.D. (2007). Onset of the Iberian upwelling along the Galician
702 coast. *Continental Shelf Research, 27*, 1759-1778.
703 Varela, M. (1992). Upwelling and phytoplankton ecology in Galician (NW Spain) rías
704 and shelf waters. *Boletín del Instituto Español de Oceanografía, 8*, 57-74.

Vidal-Romaní, J. R. (1984). A orixe das rias galegas: Estado da censtión (1886-1983). Cuardenos da Área de Ciencias Mariñas, Seminario de Estudos Galegos. Vol. 1. Ediciós do Castro. A Coruña, Spain.

Zhang, T., Fell, F., Liu, Z., -S., Preusker, R., Fischer, J., & He, M., -X. (2003). Evaluating the performance of artificial neural network techniques for pigment retrieval from ocean color in Case I waters. *Journal of Geophysical Research, 108*, 3286-3298.

Tables and graphs

727 Table 1. MERIS imagery showing the acquisition time (UTC) and mean view zenith
728 angle from west. Sea-truthing ranges of chlorophyll *a* (chl*a*), suspended particulate
729 matter (SPM), percentage of inorganic contribution to SPM and Secchi disk depth (Zsd)
730 for *ria de Vigo* (12 stations) during the two samplings.

Chl*a* (mg m^{-3})		0.03-2.65			0.03-2.72	
SPM (mg L^{-1})		1.45-2.48			1.17-3.15	
inorganic matter (%)		36-56			38-58	
Zsd (m)		2-12			2.5-7	
MERIS FR	July 03 2008	July 09 2008	July 16 2008	July 19 2008	July 22 2008	July 29 2008
Acquisition time (UTC)	10:59	11:10	10:50	10:56	11:02	10:42
View zenith angle (º)	13.5	13.0	20.7	15.3	11.7	20.7

731

732 Table 2. Percentage of pixels belonging to each cluster over the study area (*rias Baixas*),
733 obtained from classification images derived from the MERIS images used in this study.

734

Date	*ria*	Cluster#1	Cluster#2	Cluster#3
July 03 2008	Vigo	74.22	23.95	1.83
	Pontevedra	62.50	37.35	0.15
	Arousa	76.33	22.55	1.13
July 09 2008	Vigo	95.40	4.04	0.55
	Pontevedra	96.14	3.57	0.30
	Arousa	94.24	3.01	2.75
July 16 2008	Vigo	84.52	15.48	0.00
	Pontevedra	70.48	28.78	0.73
	Arousa	49.56	47.19	3.25
July 19 2008	Vigo	82.17	17.66	0.17
	Pontevedra	83.68	16.18	0.15
	Arousa	75.68	22.48	1.84
July 22 2008	Vigo	87.41	11.88	0.71
	Pontevedra	90.06	9.79	0.15
	Arousa	82.92	15.86	1.22
July 29 2008	Vigo	72.43	27.57	0.00
	Pontevedra	24.17	75.40	0.43
	Arousa	11.67	86.60	1.73

735

736

737

738 Table 3. Performance parameters for the Chl*a* neural networks tested in this study

Chl*a* model	Data base	R^2	RMS error (mg m^{-3})	Relative RMS error %
NNRB#1	Whole	0.17	0.74	93
MERIS C2R Processor		0.09	0.80	90
NNRB#2	Cluster#1	0.24	0.69	85
MERIS C2R Processor		0.09	0.80	90
NNRB#3	Cluster#1	0.70	0.46	65
MERIS C2R Processor	High quality	0.04	0.90	89

739

740

741 Table 4. Dominant atmospheric and oceanographic conditions off the *rias Baixas*

742 categorized as three different states during the upwelling cycle in summer 2008.

Period	Date	Dominant atmospheric and oceanographic conditions off *rias Baixas*
1	July 1-10	winds blowing mainly in south direction (Iw=-108) after a period of favourable upwelling winds, mostly northward surface flow
2	July 11-21	strong north winds (Iw=900), surface flow towards southwest
3	July 22-31	mainly south blowing winds (Iw=-230), southward surface flow

743

744

745

746

747

748

749

750

751

752

753 Fig. 1. A) Galician coast and bathymetry of the area. From north to south the *rias*
754 *Baixas*: *Muros y Noya*, *Arousa*, *Pontevedra* and *Vigo*. The location of the Seawatch
755 buoy station off Cabo Silleiro is shown by a black rectangle. B) Map of *ria de Vigo*
756 showing the locations of the sampling stations. The MERIS FR pixel size is presented in
757 relation to the size of the *ria*.

758 Fig. 2. Plots of chorophyll *a* fluorescence (mg m^{-3}) vertical profiles for the upper 10 m
759 of the water column in *ria de Vigo* on A) July 09 2008 and B) July 22 2008. Also I
760 would put the date actually in each panel for clarity.

761

762 Fig. 3. Regression analysis between Total Suspended Material (TSM, also termed
763 Suspended Particulate Matter) and chl*a* concentrations. ($y=1.76+0.13x$, $R^2=0.1$ and
764 sample size N=41).

765

766 Fig. 4. Classification of MERIS images derived from the study area. The 3 classes
767 identified using the FCM are shown.

768

769 Fig. 5. A) Daily upwelling index off the *rias Baixas*. The Iw in m^{-3} s^{-1} $100m^{-1}$ represents
770 the offshore Ekman flux in the surface layer. Arrows indicating the days where MERIS
771 FR images were available and numbers the different states identified during the studied
772 period and cycles the days of sampling. B) Surface currents (cm s^{-1}) recorded by the
773 Seawatch buoy station located off Cape Silleiro (42° 7.8′N, 9° 23.4′W). Data were daily
774 averaged from 0 a.m. on July 1 2008 to 12 p.m. on July 31 2008. Symbols as in Fig. 2.

775 C) Daily average of sea temperature for the month of July 2008 off the *rias Baixas*. All
776 data are means ± 1 S.D.

777

778 Fig. 6. MODIS-derived Sea Surface Temperature maps for *rias Baixas* and adjasted
779 coastal waters during the upwelling cycle of July 2008. White patches represent clouds.

780

781 Fig. 7. Chl*a* maps for MERIS FR data derived during the upwelling cycle of July 2008
782 in the study area. Land and clouds were masked and they appear with white colour.

783

784 Fig. 8. RGB MERIS (l2) FR composite image acquired on July 22 2008 over the study
785 area. Land was masked with black colour.

786

787

788

789

790

791

792

793

794

795

796

797

798

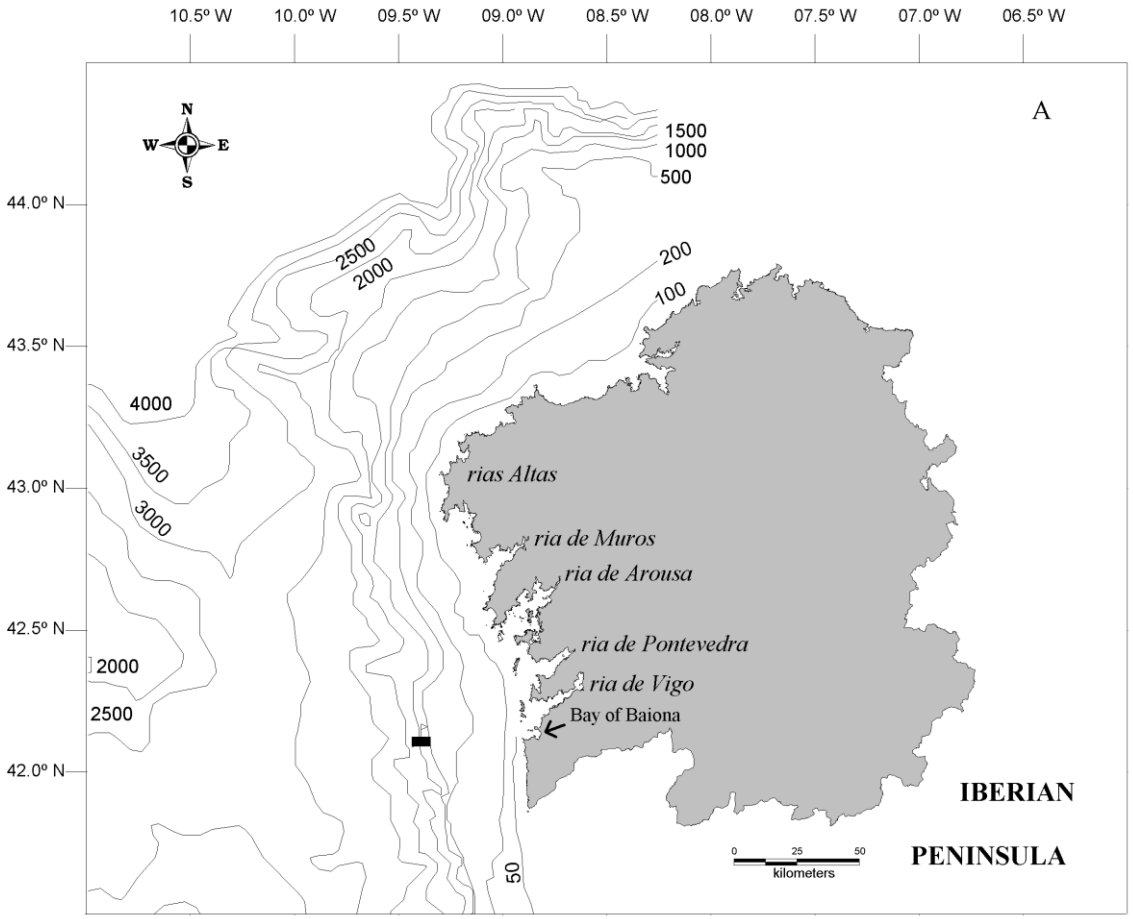
10.5º W
10.0º W
09.5º W
09.0º W
08.5º W
08.0º W
07.5º W
07.0º W
06.5º W
A
N
W
E
S
1500
1000
500
200
100
2500
2000
4000
3500
3000
2000
2500
50
44.0º N
43.5º N
43.0º N
42.5º N
42.0º N
rias Altas
ria de Muros
ria de Arousa
ria de Pontevedra
ria de Vigo
Bay of Baiona
IBERIAN
PENINSULA
0 25 50
kilometers

799

800

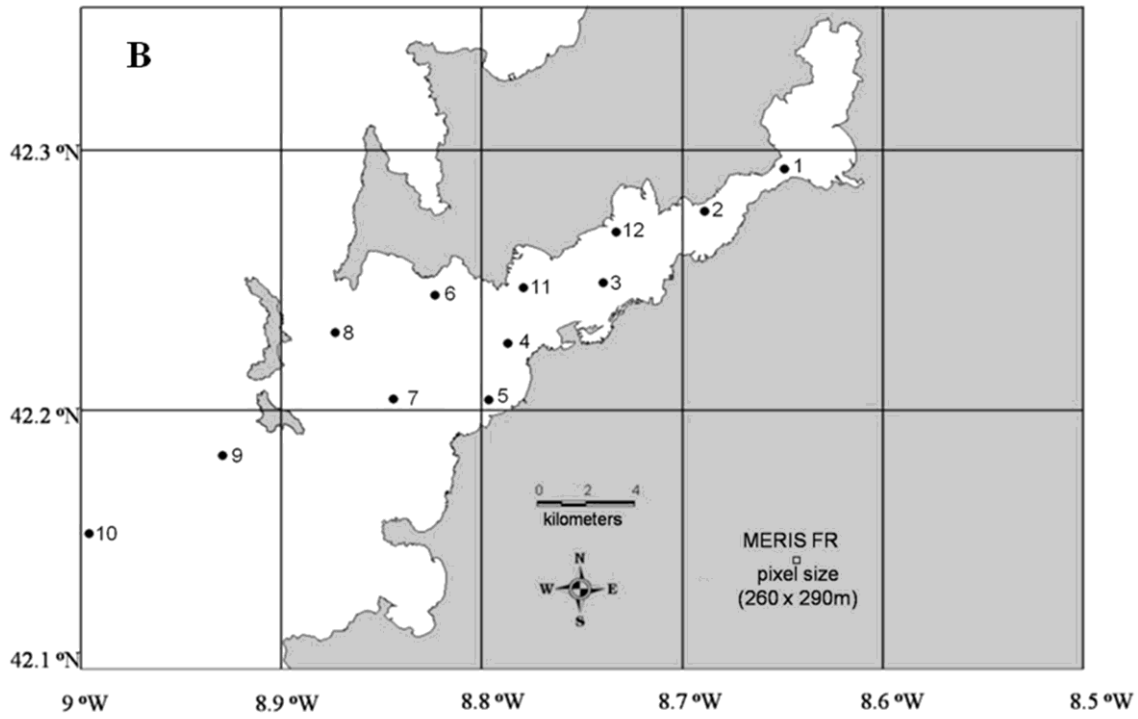
B
42.3 ºN
42.2 ºN
42.1 ºN
9 ºW
8.9 ºW
8.8 ºW
8.7 ºW
8.6 ºW
8.5 ºW
1
2
12
3
11
6
8
4
7
5
9
10
0 2 4
kilometers
N
W
E
S
MERIS FR
pixel size
(260 x 290m)

801

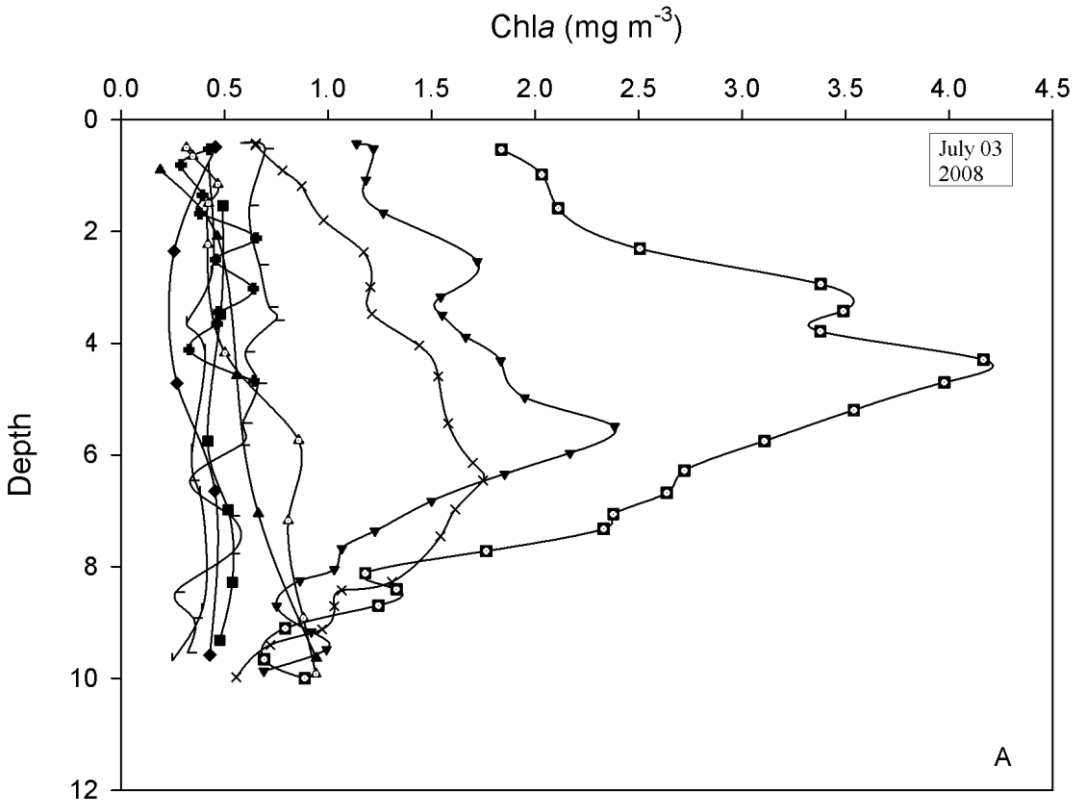
Chla (mg m-3)
0.0
0.5
1.0
1.5
2.0
2.5
3.0
3.5
4.0
4.5
Depth
0
2
4
6
8
10
12
July 03
2008
A

802

803

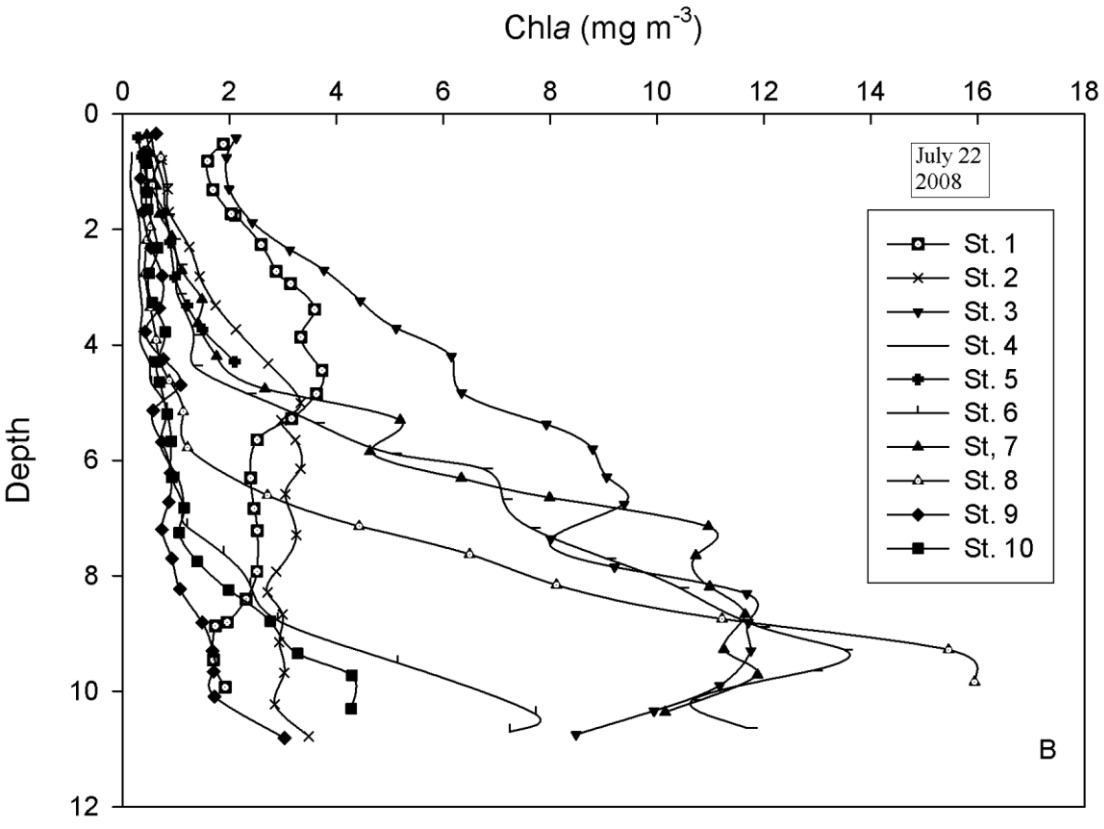
Chla (mg m-3)
0
2
4
6
8
10
12
14
16
18
Depth
July 22
2008
St. 1
St. 2
St. 3
St. 4
St. 5
St. 6
St, 7
St. 8
St. 9
St. 10
B

804

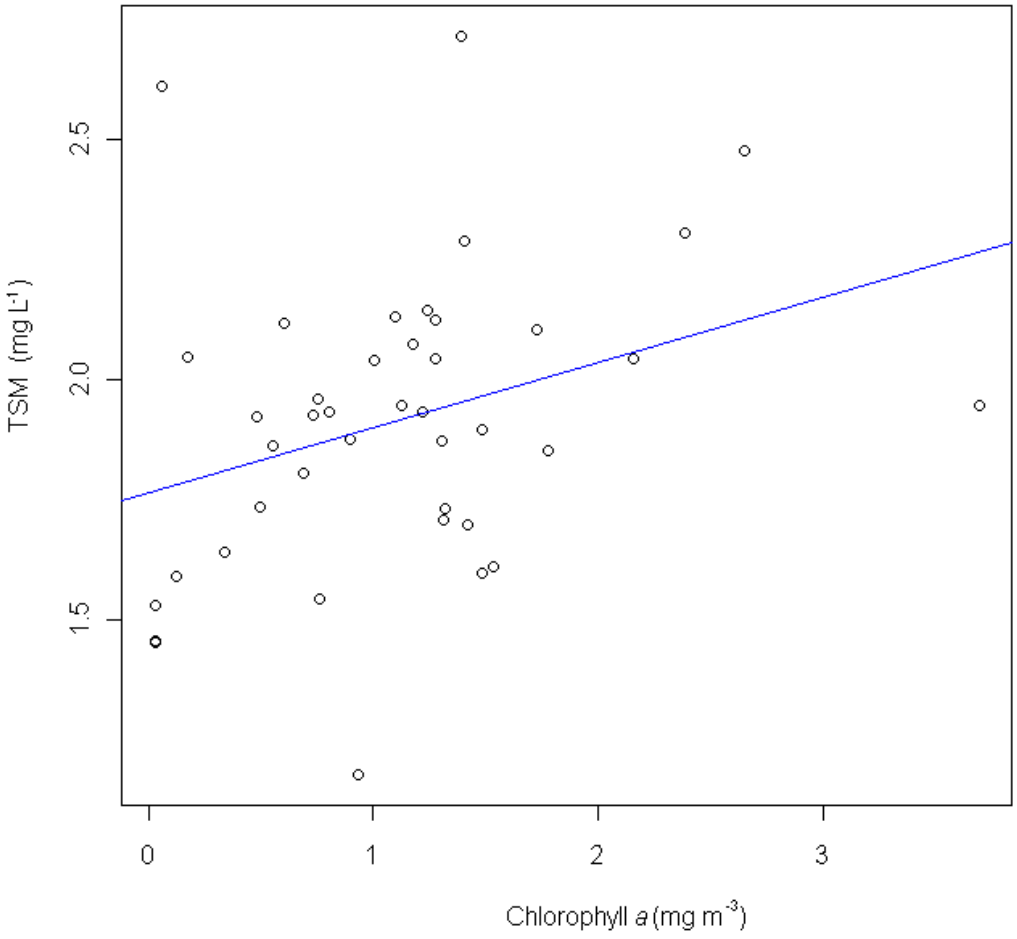

805

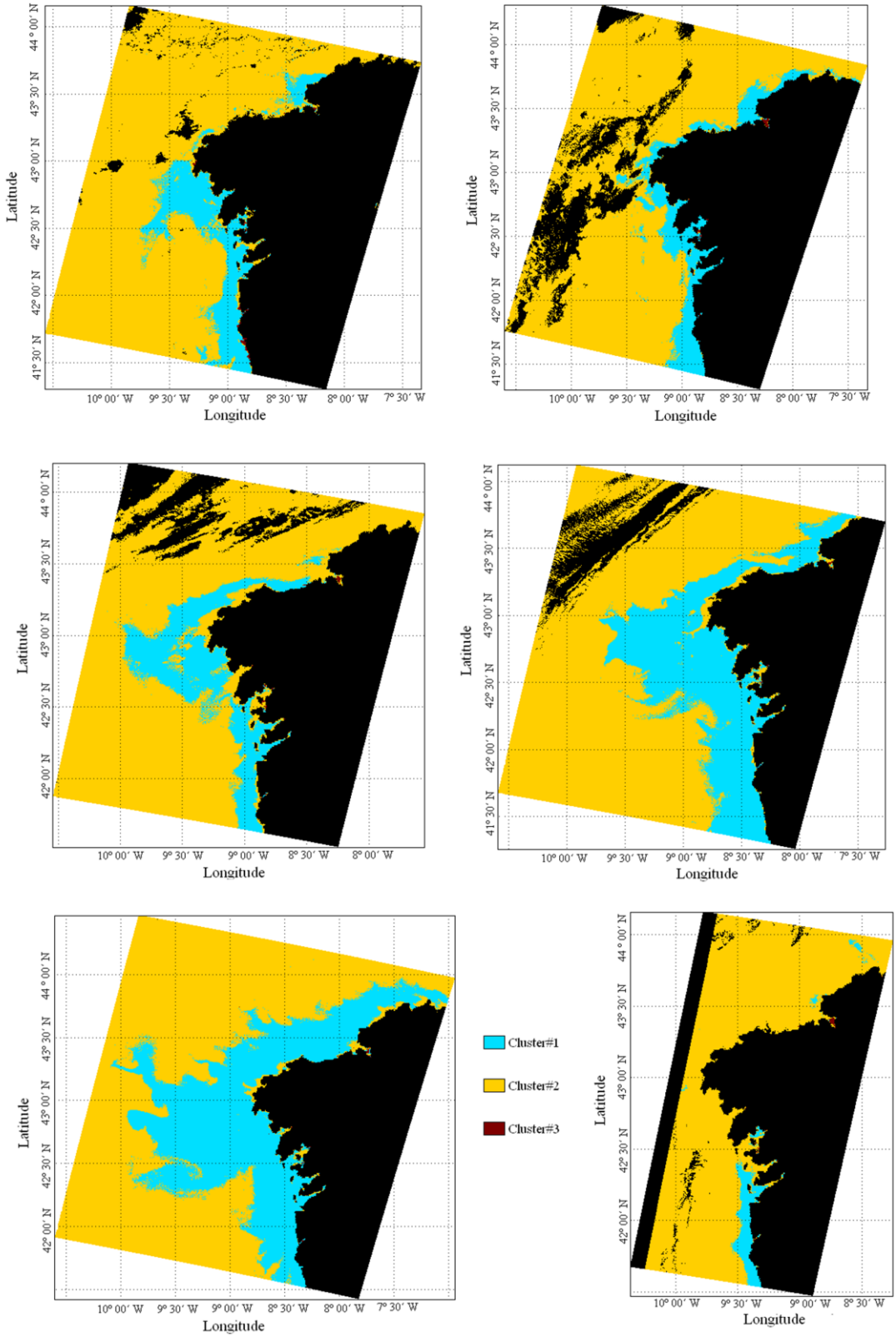

806

807

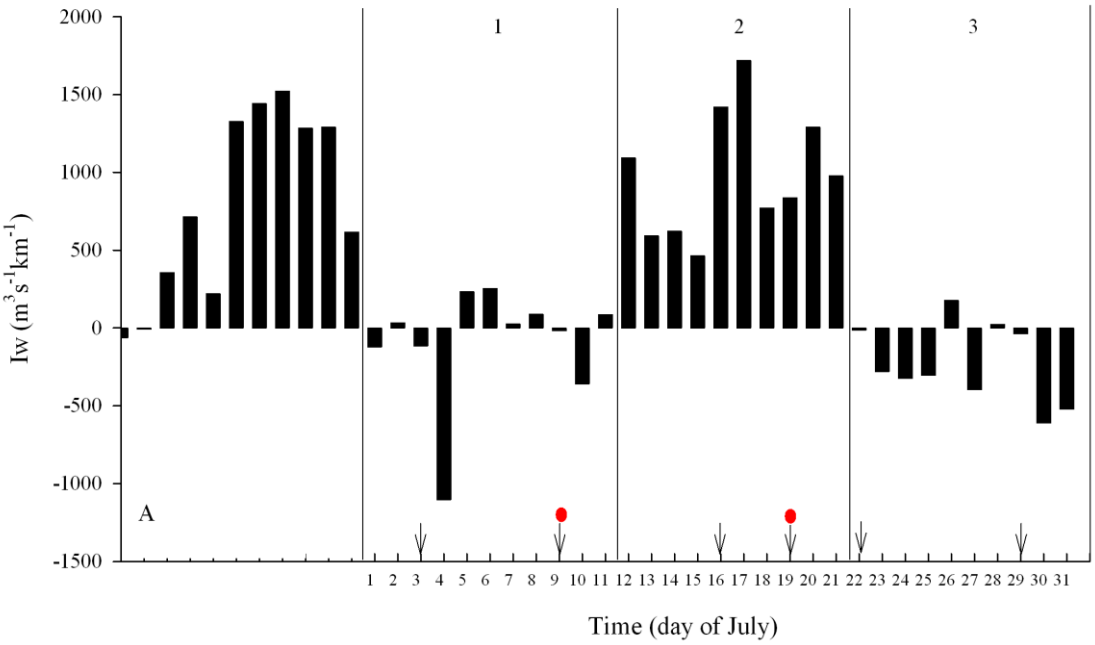

808

809

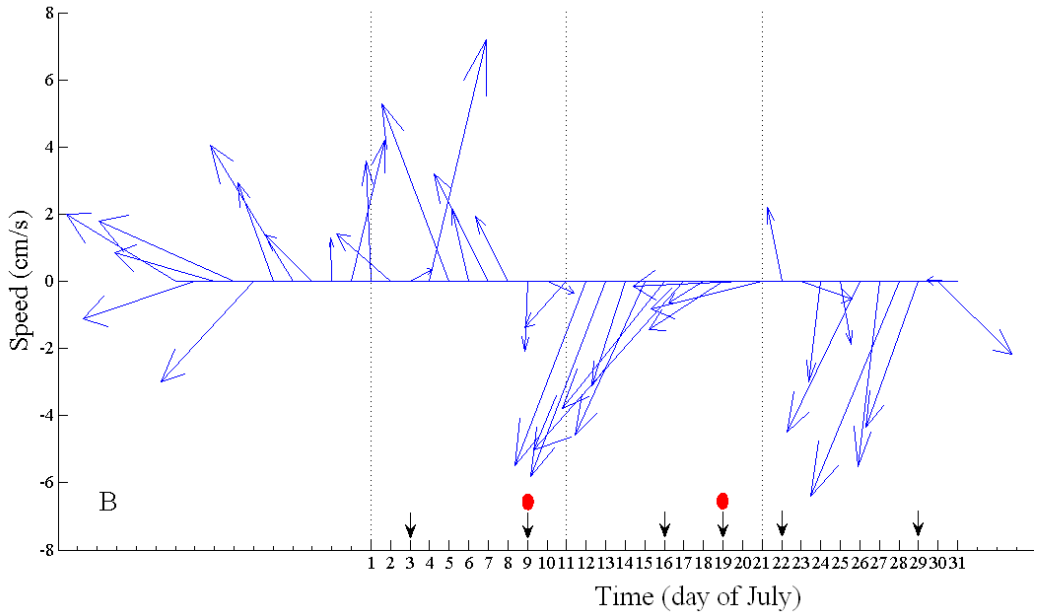

810

811

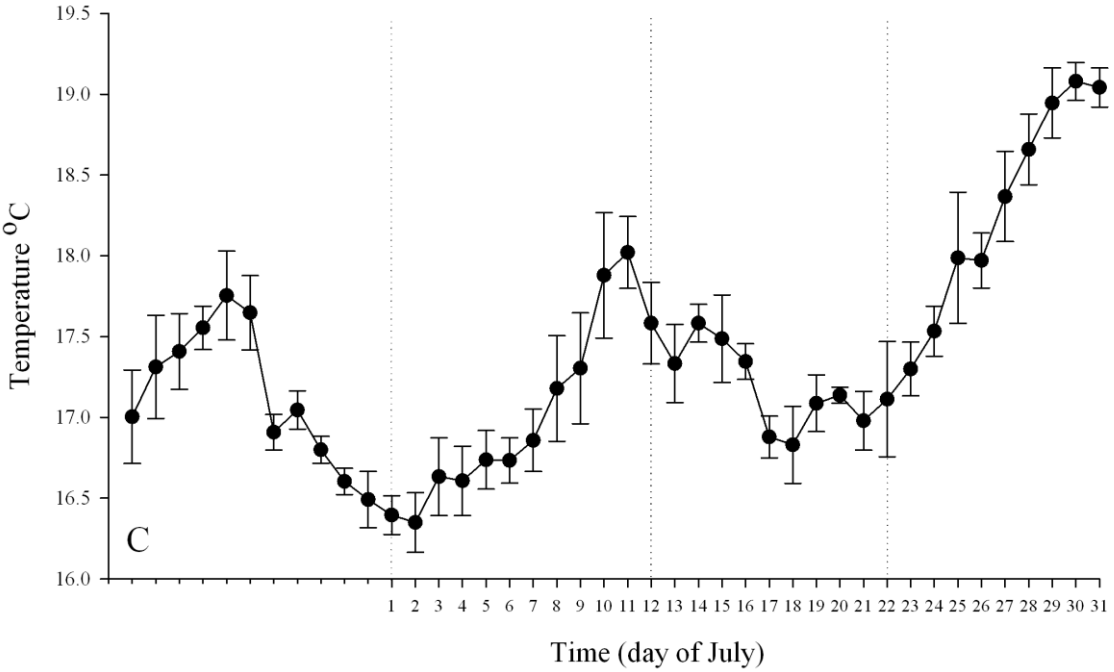
Temperature °C
19.5
19.0
18.5
18.0
17.5
17.0
16.5
16.0
C
1 2 3 4 5 6 7 8 9 10 11 12 13 14 15 16 17 18 19 20 21 22 23 24 25 26 27 28 29 30 31
Time (day of July)

812

813

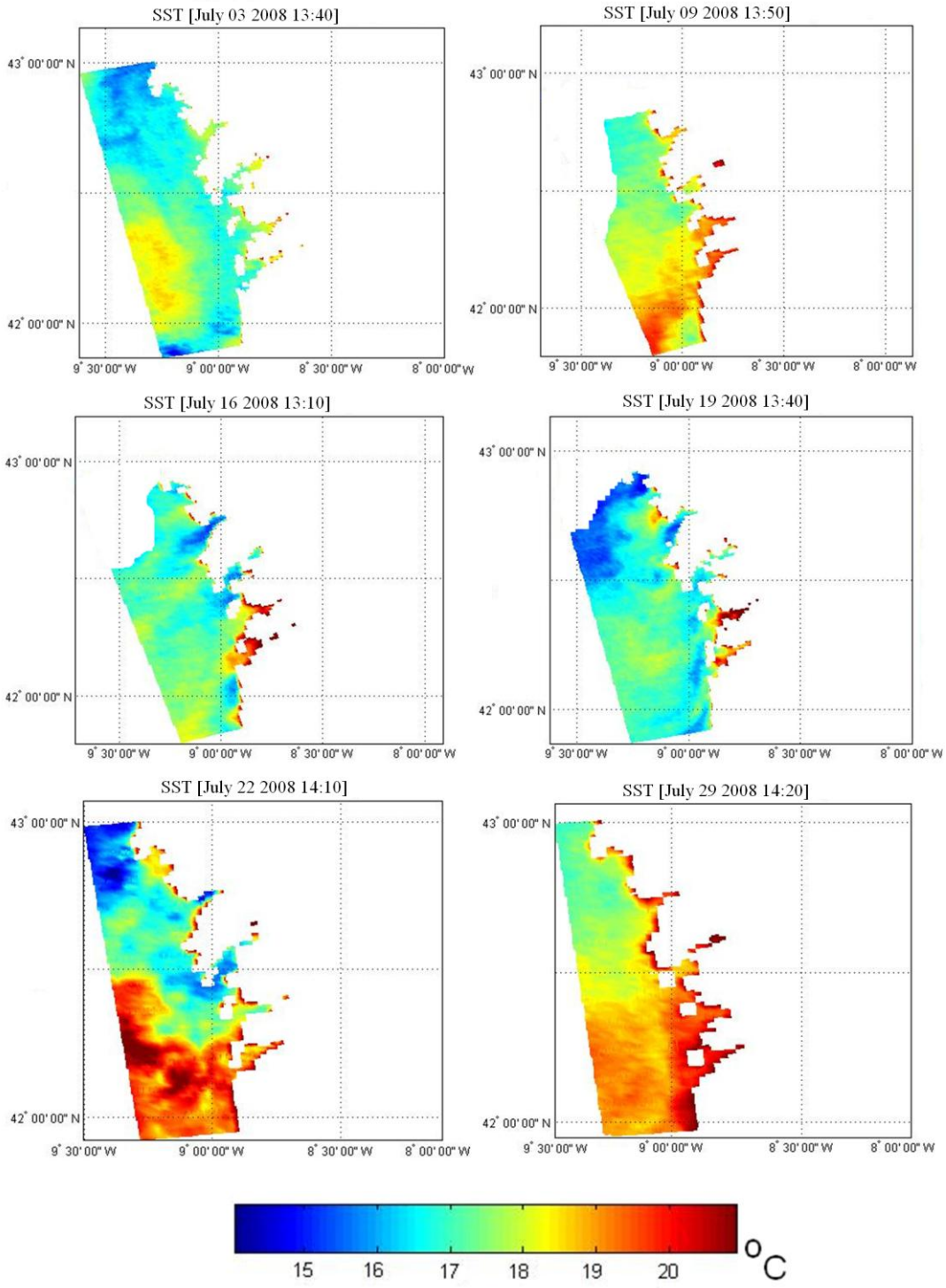
SST [July 03 2008 13:40]
SST [July 09 2008 13:50]
SST [July 16 2008 13:10]
SST [July 19 2008 13:40]
SST [July 22 2008 14:10]
SST [July 29 2008 14:20]
43° 00' 00" N
42° 00' 00" N
9° 30' 00" W
9° 00' 00" W
8° 30' 00" W
8° 00' 00" W
15
16
17
18
19
20
°C

814

815

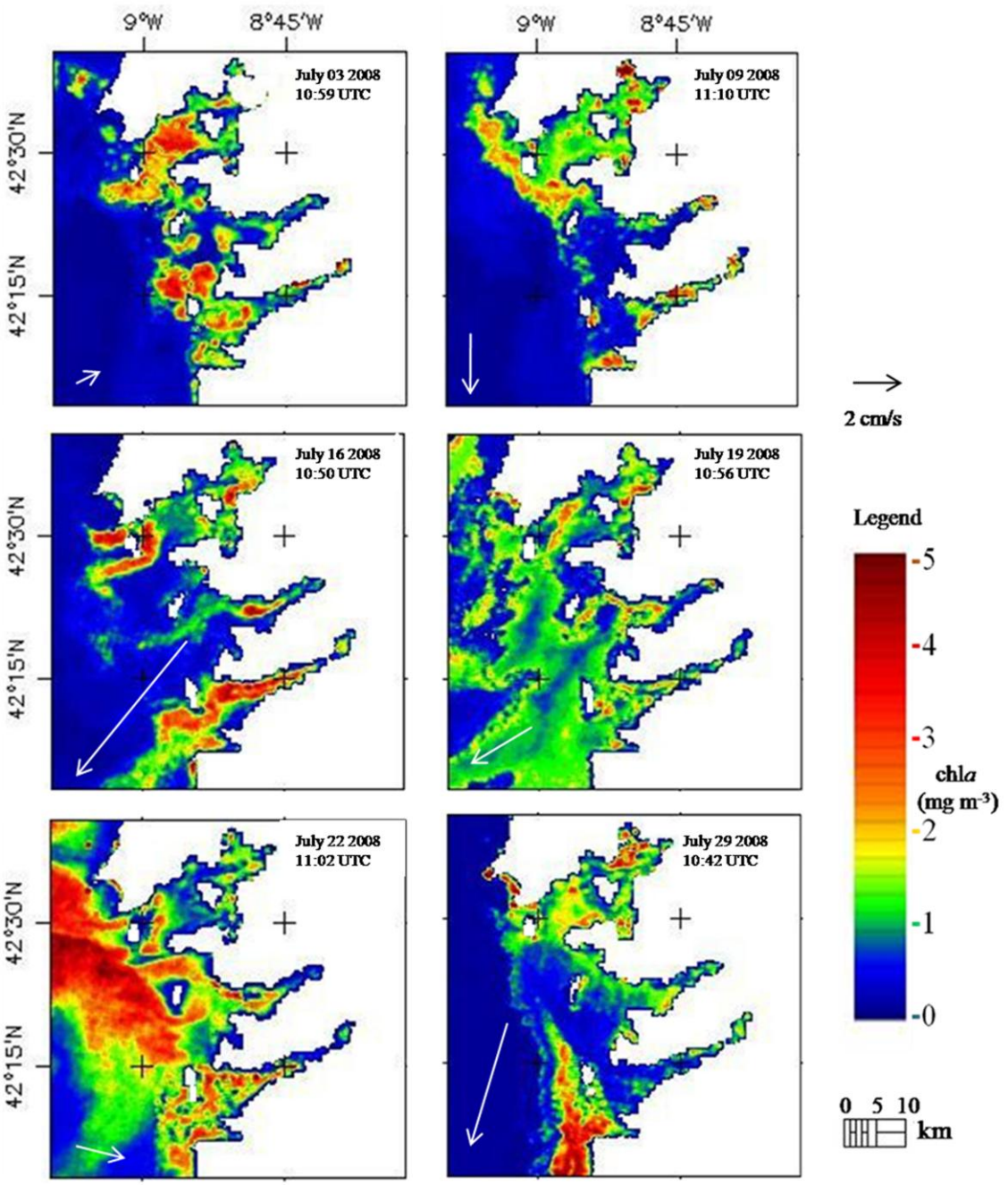
9°W
8°45'W
42°30'N
42°15'N
July 03 2008
10:59 UTC
July 09 2008
11:10 UTC
July 16 2008
10:50 UTC
July 19 2008
10:56 UTC
July 22 2008
11:02 UTC
July 29 2008
10:42 UTC
2 cm/s
Legend
5
4
3
chla
(mg m-3)
2
1
0
0 5 10
km

816

817

818

819